Mars laser hygrometer

Christopher R. Webster, Gregory J. Flesch, Kamjou Mansour, Robert Haberle, and Jill Bauman

We have designed and built a miniature near-IR tunable diode laser (TDL) spectrometer for measuring *in situ* the water vapor mixing ratio either in the Martian atmosphere or thermally evolved from Martian soil or ice samples. The laser hygrometer uses a thermoelectrically cooled single-mode distributed-feedback TDL at 1.87 μm to scan over a selected vibration–rotation line of both H_2O and CO_2 near 5327.3 cm^{-1}. A working prototype that weighs only 230 g has been built and used to generate spectra whose analysis demonstrates precision sensitivities as fine as 1 part in 10^6 by volume in 1 s or 0.1 part in 10^6 in 10 s at Martian pressures and temperatures. Absolute uncertainties of ~5% are calculated. © 2004 Optical Society of America

OCIS codes: 120.6200, 010.7340, 300.6260.

1. Introduction

NASA's recently restructured Mars Exploration Program calls for a series of highly ambitious missions over the next decade, to be achieved with relatively low mission risk and within tight cost constraints.[1] Launch opportunities in 2007, 2009, and beyond have been identified for two new mission types, named Mars Scout missions and Mars Science Laboratory (MSL) landers. The Mars Scout project will include airborne vehicles, small landers, and subsurface explorers in opportunities to implement innovative science investigations to augment primary Mars Exploration Program missions. The MSL mission is considered the gateway mission to precede the first sample return mission, scheduled to fly after 2011. The MSL will target a landing site previously selected from remote-sensing observations and will explore the Martian surface and subsurface by using a rover that will traverse at least 6 km across the planet. The laser hygrometer described here was specifically prototyped and tested for consideration for the payload of one such Mars Scout mission, Pascal, although it has wide applications for future Mars Scout and MSL missions.

C. R. Webster (chris.r.webster@jpl.nasa.gov), G. J. Flesch, and K. Mansour are with the Jet Propulsion Laboratory, California Institute of Technology, Pasadena, California 91109. R. Haberle and J. Bauman are with the NASA Ames Research Center, Moffett Field, California 94305.

Received 20 November 2003; revised manuscript received 1 April 2004; accepted 24 May 2004.

0003-6935/04/224436-10$15.00/0

A. Pascal Mars Scout Mission

As one example of the wide application of the laser hygrometer, we consider its role in the payload of the recently proposed Pascal mission. In this mission[2] a global network of 18 weather stations, each including a laser hygrometer, will operate on the Martian surface for several years, communicating by use of an orbiter spacecraft already in place, to create a detailed global picture of Martian climate and weather.[2] Each Pascal station will return a suite of meteorological information, including diurnally resolved measurements of surface pressure, atmospheric opacity, temperature, wind speed, and near-surface water vapor concentration. Panoramic cameras will supply monthly images of the Martian surface, revealing wind-related changes in surface properties. In addition, the probes will measure the thermal structure of the atmosphere and record as many as 120 images above each of the 18 landing sites as the probes descend through the Martian atmosphere.

A three-axis stabilized spacecraft will deliver 18 probe entry systems carrying the science stations on approach. A carefully engineered probe entry system design will ensure efficient packaging of all science instruments into a straightforward, lightweight station with few moving parts. Microthermal power sources, based on well-understood space flight-proved lightweight radioisotope heating unit sources, will provide the long life and thermal control of the stations. During entry, descent, and landing, each of Pascal's probe entry systems will perform acceleration measurements to determine the thermal structure of the atmosphere from ~130 to ~15 km. Below 15 km, the altitude of parachute deploy, Pas-

cal's probe entry system will then acquire ~10 color images of the surface from a faculty-supervised university student descent-imaging experiment. On the surface, pressure, temperature, water vapor, and opacity measurements will yield information on global circulation systems, regolith–atmosphere H_2O exchange, seasonal condensation of the polar ice caps, and atmospheric forcing functions. Together, these measurements will discover and characterize Martian global weather patterns, including the mass flow to and from the polar ice caps; tropical Hadley cells and thermal tides; migrating midlatitude weather systems in each hemisphere; topographically controlled stationary waves, low-level jets, and storm zones; and the planet's most impressive weather phenomenon, raging dust storms.[2] In addition, the descent-imaging experiment will provide a better understanding of the diversity of Martian terrains, which will be a benefit for site selection activities for future rover and sample return missions.

B. Martian Water Cycle

Mars is a rocky planet whose surface features are determined by past volcanism, crustal motion, impact cratering, and continual dust storms.[3,4] Polar caps made from frozen CO_2 and H_2O are visible from Earth, growing and receding seasonally. The planet is believed to have experienced huge water floods some 3 to 4 billion years ago but now has a dry surface. Martian weather controls the movement of dust around the planet, the exchange of water between the surface and the atmosphere, and the seasonal cycling of CO_2—the dominant atmospheric constituent—into and out of the polar regions.[3]

Water vapor in the Martian atmosphere has been observed from orbiting spacecraft and Earth-based telescopes.[5] The observed variation in the abundance of water vapor in space and time within the Martian atmosphere had suggested the existence of surface sources and sinks.[6] We now know from the latest measurements from the Mars Global Surveyor and the Mars Odyssey spacecraft experiments[7] that Mars has an active hydrological cycle in which water is exchanged between the surface and the atmosphere on seasonal and possibly diurnal time scales. Water reservoirs at both the north and the south poles are identified, as large subsurface reservoirs close to the surface, of water ice mixed into the soil only a meter below the surface.[7] Previously the residual north polar ice cap had been identified as the source of water for the north polar summertime maximum,[8] but no such reservoir had been detected at the south pole even though a high-latitude summertime maximum had also been seen in the southern hemisphere.

Because water is a critical component in biological activity, discovery of the location of its reservoirs and partitioning among vapor, liquid, and solid phases is a high-priority objective for current and future Mars missions that address the possibility of life on Mars.[1] It appears that liquid water has been on the surface in the relatively recent past in the form of seepage gullies.[9] Models indicate that there are certain places and times on present-day Mars that thin films of solar-heated liquid water could exist temporarily, given the right circumstances.[10] Whereas liquid water seems an unlikely possibility for Mars,[11] these recent observations and theoretical developments argue against ruling it out completely.

C. Measuring Water on Mars

Previous measurements of atmospheric water vapor on Mars were made either from orbit or from Earth-based telescopes, but the higher precision and accuracy of *in situ* measurements are needed to determine the atmospheric and subsurface abundances, to detail the nature of surface–atmosphere exchange processes, and to identify possible local sources. Despite the huge success of the Mars exploration rovers Spirit and Opportunity, no direct *in situ* measurements of water have yet been made on Mars. In considering possible *in situ* water measurement techniques suitable for Mars at low pressures [7–10 mbars (700–1000 Pa)] and temperatures (170–220 K) at a few parts per million by volume (ppmv), we turn to successful techniques used on Earth to measure *in situ* stratospheric water vapor at 3–50 ppmv at similar low pressures (tens of millibars) and only moderately higher temperatures (190–280 K). These methods (see Ref. 12 for a review of techniques) include frost point detection on chilled mirrors, vacuum ultraviolet (Lyman-α) absorption and fluorescence, tunable diode laser (TDL) spectrometers such as the one described here, and a variety of humidity sensors carried on balloon-launched radiosondes. For these humidity sensors, carbon hygristors and thin-film capacitors are most common, but carbon hygristors are highly unreliable and do not function at all at temperatures below ~220 K. Thin-film capacitors marketed as Humicap and used on Vaisala and Meisei radiosondes are successful for tropospheric measurements but are not capable of measuring water vapor at saturation mixing ratios below ~220 K. For Mars, then, carbon hygristors and thin-film capacitors could not provide measurements.

For Mars application, chilled mirror frost point hygrometers or Lyman-α hygrometers could in principle be made from low mass, volume, and data rates approaching those of TDL hygrometers. However, TDL spectrometers offer several distinct and important advantages over frost point and Lyman-α hygrometers, which include faster time response and increased precision, producing measurements in fractions of a second, an important factor for water flux measurements; lower power requirements for a more efficient light source; and a simpler, more compact, and more robust optical system. Furthermore, the TDL spectrometer makes direct, noninvasive measurements of water (Lyman-α hygrometers dissociate water and measure the OH produced) and cannot be outperformed for low mass optical head and electronics. An additional advantage of the spectrometer described here is its ability also to record or use in-

formation from the CO_2 spectral line adjacent to that of water.

D. Laser Hygrometers: Instrument Requirements and Heritage

We have developed several new laser hygrometers for measuring water vapor both in the Earth's atmosphere (for the aircraft ER-2, DC-8, and WB-57) and on the surface of Mars [the Mars Volatiles and Climate Surveyor (MVACS) polar lander, the Mars Organic Detector (MOD), and the Mars Scout]. All these instruments are based on measuring water absorption by the 1.37-μm rovibrational transition. A group of scientists at the Jet Propulsion Laboratory[13] has over the past 20 years developed laser spectrometers for Earth (aircraft and balloon), Titan (Cassini probe, not selected), and Mars (Mars98, two instruments on a failed payload; Mars 2007 MOD TDLs). In more than 320 aircraft and balloon flights the group has demonstrated the high sensitivity of tunable laser absorption spectroscopy for *in situ* measurement of atmospheric gases in both the near-IR (1–3-μm) and the mid-IR (3–8-μm) wavelength regions. The two miniature *in situ* gas spectrometers built for the Mars 98 Surveyor's MVACS Lander payload, and the Mars 2007 MOD are based on room-temperature TDLs at near-IR wavelengths (1–2 μm) for measurement of atmospheric H_2O at 1.37 μm and of isotopic CO_2 at 2.04 μm.[14]

In this paper we report details of a laboratory prototype spectrometer that could measure water vapor in a configuration accommodated on the Pascal probe of the Mars Climate Network Mission. The science requirements for this mission determined that we should be able to measure water vapor within a precision of 1 ppmv at a nominal surface pressure near 7 mbars, which would be equivalent to 2.3×10^{11} molecules cm^{-3}, i.e. down to a surface water frost point temperature of ~170 K.

E. Tunable Laser Sources and Absorption Spectroscopy

Room-temperature (TE cooler) TDL sources of high spectral purity (single mode) and high output powers (5–50 mW) are now available in the near-IR region where molecules such as H_2O and CO_2 have sufficiently strong IR absorption cross sections. For wavelengths in the 1–2 μm range, the JPL's Micro-Devices Lab has produced single-mode distributed-feedback (DFB) devices that have been tested and flight qualified for the Mars MVACS lander payload of the Mars 98 Surveyor mission for measurement of atmospheric and evolved H_2O at 1.37 μm.[14] Laser sources at 1.87 μm have also been made by both the Micro Devices Lab and Nanoplus in Germany but have not been flight qualified in any way. Pushing operating wavelengths of these devices beyond 2.5 μm is proving difficult, although a stronger water band exists near 2.7 μm. For the strong mid-IR water band near 6 μm, quantum cascade (QC) laser sources are required.

QC lasers are new mid-IR semiconductor laser sources [invented in 1994 (Ref. 15)] that are fundamentally different from TDLs.[16,17] Rather than depending on the electronic bandgap of materials, the QC laser results from the application of quantum engineering of the electronic energy levels. QC laser emission results from intersubband transitions within the conduction band of a cascaded InGaAs–InAlAs multiple-quantum-well structure lattice that has been matched to an InP substrate by molecular beam epitaxy[16]; the output wavelength is determined by quantum confinement, i.e., by the layers' thickness in the active region rather than by the bandgap of the material.[15,16] Progress in QC laser development has been very rapid: Cryogenically cooled cw DFB QC lasers were recently flown on high-altitude aircraft to measure CH_4 and N_2O in the Earth's stratosphere,[17] and room-temperature cw operation of QC lasers (at 9 μm) has now been achieved,[18] with cw output powers of a few milliwatts.

Tunable laser absorption spectroscopy is widely recognized as a direct, noninvasive, simple measurement technique that is known for its high sensitivity (better than parts-in-10^9 accuracy) and specificity.[19] With wavelength-modulation techniques, minimum-detectable absorptions as small as 2 parts in 10^6 are possible, with 2 parts in 10^5 readily achieved in flight experiments. For reasonable path lengths this translates to parts-in-10^9 sensitivities for numerous species in the mid IR and to tens of parts in 10^9 in the near-IR region. (These numbers depend specifically on the gas and conditions of interest.)

2. Mars Laser Hygrometer

A. Laser Choice and Results of Sensitivity Trade-Off Study

Three candidate wavelength regions[20] were considered in this study, two regions in the near IR at 1.37 and 1.87 μm and a mid-IR region near 5.9 μm (see Fig. 1). The mid-IR region is ~20 times stronger than the near IR, but room-temperature (TE-cooled) QC lasers are not yet flight qualified.

Concerning the choice between using a near-IR TDL at 1.37-μm wavelength or a mid-IR QC laser at 5.9 μm, we identified the trade-off factors. Besides providing access to weaker rovibrational lines, the near-IR region is the location of a significant heritage of space-flight experience and of lasers that have been flight qualified. The mid-IR region, however, has no flight qualification but does offer an increase in line strength by a factor of 20. An alternative line at 5327-cm^{-1} or 1.877-μm wavelength exists that is nearly twice as strong as the 1.37-μm line, with the added advantage that it conveniently follows a CO_2 line that can be used for pressure measurement or normalization. Using the alternative line reduces the advantage of the mid-IR to only a factor-of-10 greater sensitivity but retains the near-IR heritage and laser flight qualification already made. (Although we may need to extend the wavelength range of the InGaAs detector, this is an unimportant change.) Regarding laser availability, other commercial companies[21] have put significant amounts of

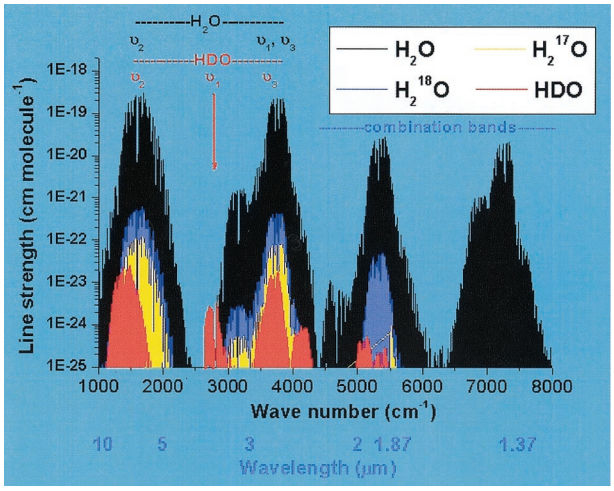

Fig. 1. Vibration–rotation line positions and intensities that make up the main absorption band regions of water and its isotopologs $H_2{}^{16}O$, HDO, $H_2{}^{18}O$, and $H_2{}^{17}O$. Source: HITRAN 2000-line listing.[20]

money into securing a good source of the exact wavelength for measuring water in gas pipelines that contain huge amounts of CH_4. Thus, whereas these companies have focused on finding a good water line in a forest of CH_4 lines (1.37 μm does not work), the possibility of also measuring CO_2 in this region had not been considered. The JPL's Micro Devices Lab is committed to developing lasers at this wavelength.

Thus, for Mars applications, use of the region near 1.877-μm is recommended; there we retain the flight qualification and heritage advantage, we have an abundant source of existing good lasers, and we always also get a CO_2 line measurement, which is an excellent calibration standard in every spectrum (Fig. 2). Of course, to make our gas measurements we need pressure and temperature to determine mixing ratios. So we can either use CO_2 as a massless pressure gauge (continuous simultaneous calibration of the H_2O absolute accuracy) or we can report CO_2 mixing ratios to 0.1% estimated precision for 96% CO_2.

B. Optomechanical Configuration

It was estimated that, in order to achieve the sensitivity demanded by the Pascal mission, we should use a Herriott cell[22] (H cell) with a base optical path of ~50 cm. The final design configuration (Figs. 3 and 4) was chosen as a compromise between minimizing the number of passes and fitting the length of the cell within the 4-in. (10.16-cm-) diameter probe. The final H cell design parameters are given in Table 1. Although we planned to use a bar mirror configuration, we eventually opted for the circular mirror design based on the results of g-force analysis.

The all-aluminum H-cell housing is a ventilated structure that provides support and spacing for the optical elements of the instrument. There are two spherical mirrors, mounted at opposite ends of the cylindrical portion of the housing. The mirror located near the center of the housing has an off-center hole that provides access to the cell for both the source and the return laser beams.

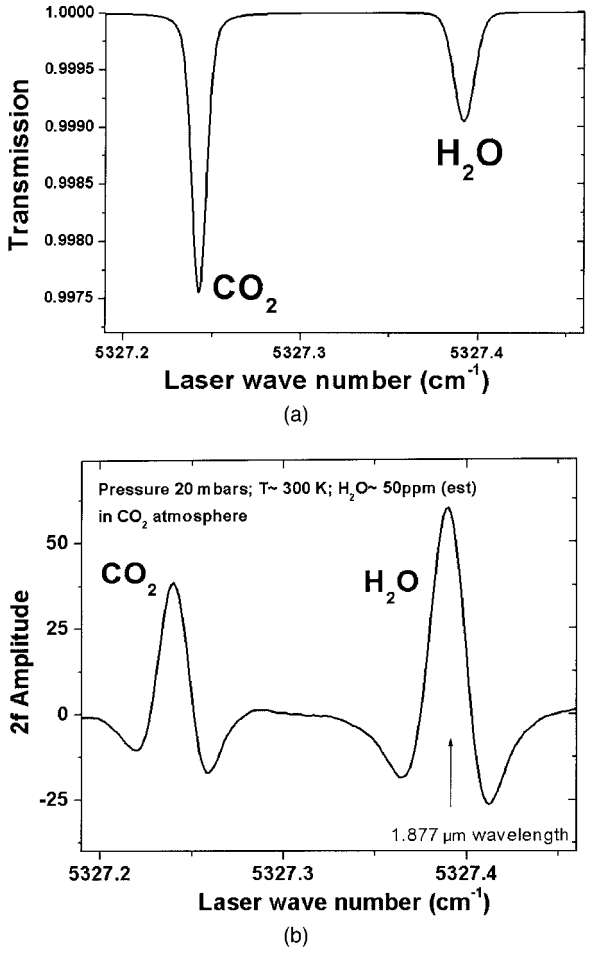

Fig. 2. (a) Spectral simulation of the direct absorption spectrum in the region near 1.87 μm by use of the HITRAN 2000 data[20] calculated for conditions appropriate for the Martian surface, namely, 7-mbar pressure, 200-K temperature, and an atmosphere of 96% CO_2 and 20-ppmv water vapor. (b) Actual spectral data produced by the MLH in the same region. The spectrum results from second-harmonic detection at 15.62 kHz in 20-mbar CO_2 and 50-ppmv water vapor.

The mirror at the end of the cell is secured with the bonding agent RTV to the far mirror mount, which in turn is epoxied into the H-cell housing. The mirror near the center of the housing is potted with RTV into the near mirror mount ring, which is then secured to the housing body with RTV. RTV was chosen as a bonding agent to accommodate the difference between the temperature coefficients of mirror and aluminum.

The laser–detector mount (Fig. 4) provides a temperature-stabilized structure that holds the laser, the detector, and their respective lenses. The detector lens (in the shorter mount) is fixed in focus and lateral movement. The laser lens is mounted in the laser lens mount and the laser lens thimble, which provide the ability to focus and move the lens laterally.

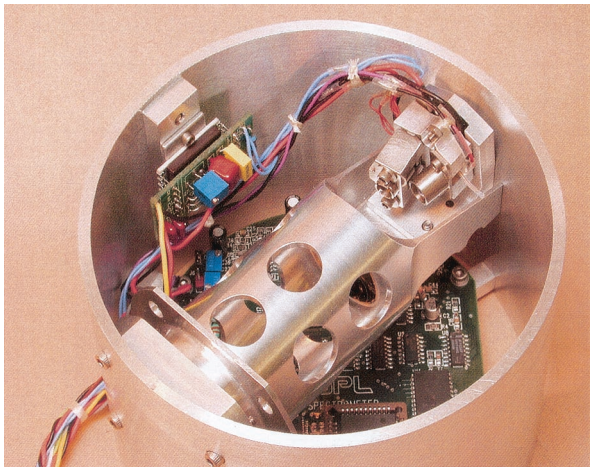

Fig. 3. Complete MLH mounted in a section of the 10-cm-diameter cylindrical body of the probe.

Fig. 4. Optical head of the MLH, which comprises a TE cooler mount with laser and detector and an H cell. The cylindrical geometry offers superior resistance to g loading, and the holes in the cylinder side provide both air venting and light weighting.

The rectangular end of the H-cell housing (Fig. 4) provides a mounting platform for the active optics assembly. The assembly consists of the structural mount (hot plate) and the laser–detector mount (cold plate), which are separated by a thermoelectric cooler (see Subsection 2.C below for a description of the thermal control). There are four glass–epoxy rods that provide registration between the hot plate and the cold plate as well as preventing shear forces from being applied to the cooler. The plates are isolated from each other thermally and electrically.

The rectangular end of the H cell is secured to the wall of the spacecraft with a single 8-32 bolt, which will be in shear during acceleration. A common cap screw has been used in the delivered instrument; however, the final design will require a specialty bolt or a sleeved bolt to prevent the threaded portion of the bolt from receiving shear forces. The cylindrical end of the H cell floats within the enclosure adaptor mount, which is secured to the wall of the spacecraft with four 4-40 bolts. The cylinder is free to move axially within the mount but is constrained laterally. A registration pin in the adaptor mount rides in a slot in the cylinder, preventing rotation. Common cap screws have been used in the delivered instrument; however, the final design will require specialty bolts or sleeved bolts to prevent shear forces on the threaded areas of the bolts.

The electronics board (Fig. 5) was supported by an X-shaped aluminum bracket designed to brace the board to survive a 1000-g impact. Figure 5 shows the configuration with the probe traveling out of the page toward the reader. This bracket is secured with four bolts. The prototype instrument was designed to survive a single, nonresonant 1000-g acceleration perpendicular to the axis of the cell.

C. Electronics and Signal Processing

Temperature stabilization of the laser–detector optical head is important to ensure that the spectral lines

Table 1. Laser Hygrometer H-Cell Specifications

Mirror spacing	55.28 mm
Radius of curvature	80.1624 mm
Focal length	40.0812 mm
Mirror diameter	25.400 mm
Mirror hole diameter	3.00 mm
Mirror edge thickness	3.81 mm
Mirror material	Zerodur
Surface coating	Gold on chrome, Al_2O_3 overcoat
Total path length	55.27 cm
Optical configuration	10-pass
Symmetry	C-3
Rotation angle (theta)	72 deg counterclockwise as viewed from laser
Spot pattern diameter, nominal	1.905 cm
Injection hole location: R-L centered	3.0 mm above mirror center
Vertical injection angle	(−)6.7898 deg (down)
Horizontal injection angle	(−)9.3067 deg (left)
Laser and detector spacing from injection hole, measured normal to back of mirror	3.1 cm
Laser to detector horizontal spacing	1.0155 cm
Laser detector vertical distance above injection hole	0.3691 cm

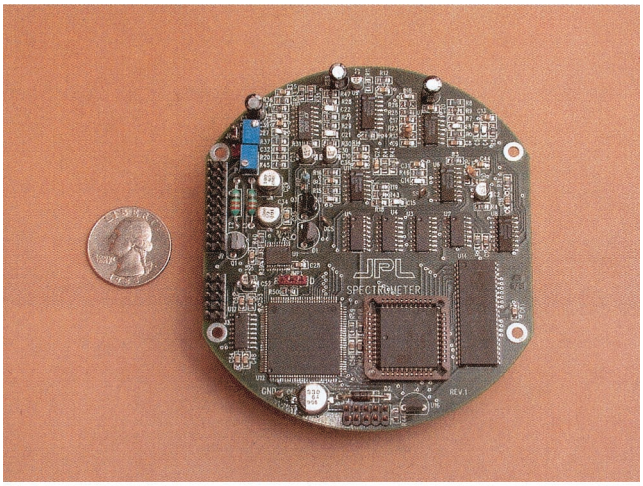

(a)

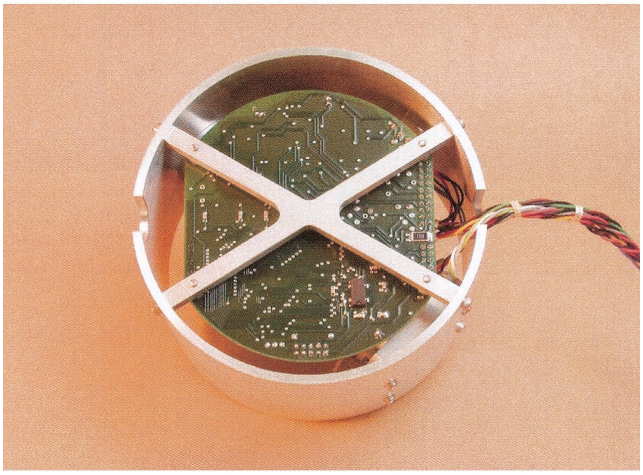

(b)

Fig. 5. (a) JPL-developed HC12-based microcontroller board, including laser drive and signal-processing electronics. (b) X-mounting configuration for mechanical support.

(H_2O and CO_2) remain well within the current ramp window and do not drift out of range; too wide a current ramp will unnecessarily reduce the duty cycle of spectral data points. Temperature stabilization is therefore achieved with a thermoelectric cooler (TEC) based on the Peltier effect that can therefore provide heat or cooling as needed. As they are in the thermoelectric cooler (TEC) used in the MVACS TDL spectrometer design,[14] laser and detector temperatures are held constant to ± 0.01 °C by a hybrid controller circuit provided by Hytek Microsystems, Inc., Carson City, Nevada, configured for proportional-integral-derivative operation to minimize overshoot on power-up. This circuitry also has compensation for the finite thermal conductivity of the aluminum mount block. Because the laser–detector set points near 0–20 °C are significantly above the Mars ambient temperatures, the TEC will be operating primarily as a heater on Mars. It is estimated that the TEC and controller can provide enough power to maintain stabilization throughout the Martian day. Although in our lab demonstration a tiny board provides the Hytek controller circuitry separate from the main electronics, the TEC electronics is included in a more recent version based on the 8051 microcontroller (see below).

The Mars Laser Hygrometer (MLH) electronics board is a four-layer, 4-in. circular circuit board that handles TDL current control, housekeeping data collection, signal processing, and downlink communication. At the heart of the electronics board is a local CPU that allows for a more intelligent sensor that is capable of real-time signal processing, in-memory averaging of spectra, and even change of operating modes through uplinked commands. Although results presented in this paper are based on a Motorola HC12A4 16-bit, 8-MHz microcontroller with 4 kBytes of on-board electrically erasable programmable read-only memory, we have also designed and built a flight-qualified, radiation-hardened board of the same dimensions but based on the 8051 microcontroller.

The MLH is a TDL spectrometer that employs both direct and second-harmonic detection. The technique is discussed fully by Webster *et al.*[19] The scan rate is set at 3.84 Hz (0.26 s), and the laser source is modulated at 7.81 kHz. Although these two values are hard wired, the remaining scan parameters (starting current, ramp amplitude, modulation amount, phase shift, and laser-off interval) are completely adjustable. Values are currently hard coded in software for turnkey operation, but they could be changed through uplink commands in real time. This might be useful in the event that a change in measurement strategy is needed or if the optimum operating temperature of the laser has changed. Currently such uplink commands are not implemented, but there is no technical barrier to prevent this from being done.

Pressure and temperature are necessary to turn the $2f$ spectra into volume mixing ratios. The MLH uses a SenSym ASCX15AN pressure gauge to measure pressure and thermistors to measure temperature. Both are read with a 12-bit MAX 147 analog-to-digital converter connected to the Motorola HC12 microcontroller's serial peripheral interface. (With some clever programming, we are actually able to get 13 bits from the analog-to-digital converter). Pressure and temperature are recorded at the end of each scan.

Having a local CPU allows us to process the spectra in real time. Pattern matching algorithms are used to send down only the salient line shape information. First, the temperature stabilization produces line center positions that are reliable to within a few linewidths. We look over this predetermined region to find the local maximum of the $2f$ signal at line center and record both its value and its laser scan index. We then look to the right and to the left to find the two minima that correspond to the $2f$ lobes and record their values and indices. Finally, we identify two additional points that corresponding to (say) two or three times the peak-to-lobe separation to provide a baseline for use in estimating power at line center.

Table 2. Data Rate Inventories for an Entire Spectral Scan and an Onboard Processed Scan

Entire Spectral Scan		Processed Spectral Scan	
Component	Bytes	Component	Bytes
512 points (direct spectrum)	1024	5 points in the direct spectrum	10
512 points (2*f* spectrum)	1024	5 points in the 2*f* spectrum	10
		Indices of these 5 points	10
Pressure and temperature values	8	Pressure and temperature values	8
5-V sense line voltage	2	5-V sense line voltage	2
Total number of bytes	2058		40

Representing a spectrum with only a few points yields a huge savings in the amount of data to be downlinked (see Table 2). Thus a 2-orders-of-magnitude improvement in bandwidth usage is achieved.

The local CPU also gives us flexibility in outputting data. For example, it might be desirable to send down an entire spectrum occasionally to check for the effects of electrical noise or optical fringing, or for calibration purposes. The information in that scan could be applied, if necessary, to subsequent real-time processed data. Although the Motorola HC12 microcontroller's serial ports can operate at a variety of line speeds, it is currently set for 9600 band, the likely data rate of the main payload computer.

The Motorola HC12 microcontroller is not available in a commercial radiation-hardened package because achieving such a package would make the space qualification process difficult and unnecessarily expensive. To address this problem we designed a new TDL spectrometer that uses only approved parts from the NASA parts selection list.[23] The new design uses a radiation-hardened UTMC 8051 microcontroller and is functionally equivalent to the Motorola HC12 based model but has two important improvements. We increased the resolution of the analog-to-digital converters from 12 to 16 bits, and we increased the laser scan rate from ~4 to 10 Hz. The 8051 microcontroller is widely deployed in spacecraft instrumentation. We built a breadboard version of this new design, using commercial parts (but equivalent to the space-qualified parts in form, fit, and function), and early testing has been successful. The protoflight version is currently being constructed and will undergo full thermal and vibrational testing this year.

The MLH electronics represent a great improvement over the circuits used in the flight laser drive and signal-processing circuits for earlier planetary instruments such as the Mars98 MVACS Thermal and Evolved Gas Analyzer or the Human Exploratory and Development of Space advanced life sciences system for the DS-2 microprobe. Those systems employed a novel approach for controlling laser current by storing the current ramp values in a ROM and then playing them back with a counter, incrementing through the ROM addresses.[24] However, the lack of a local processor with RAM limited the scan rate to that at which the lander could receive the serial data, which at 9600 baud was 2.79 s. The shortest possible scan rate is always desirable, reducing the possibility of the environment's changing significantly in the middle of the measurement. These systems also suffered from not having their own pressure or temperature measurements; for absorption lines with strong temperature-dependent parameters, this is of serious concern. Finally, as these systems could not process data locally, there was no choice but to send down the entire spectrum for each and every scan, requiring significantly more telemetry bandwidth.

D. Instrument Performance Results

Sensitivity measurements were performed at two wavelengths, 1.37 and 1.87 μm, in turn. For these, the laser hygrometer was placed in a vacuum chamber initially filled with dry CO_2 and pumped down to a nominal ~7-mbar pressure. By having enough water remaining that the direct absorption signal could be measured (8% at 1.87 μm and 15% at 1.37 μm), we could extrapolate the achieved signal-to-noise ratio to predict the minimum-detectable mixing ratio for each case. As expected, optical interference fringes limited the attained signal-to-noise ratio at each wavelength. The laser is scanned through the line at a rate of 3.84 Hz, or 0.26 s/scan.

The 1.37-μm DFB laser (SN TO5244) made at the JPL by the MicroDevices Lab scanned single mode over the water line at 7299.449 cm^{-1} with a drive current near 150 mA and at a temperature of ~10 °C. Output power was ~10 mW cw. Optical alignment was verified with an IR detection card and by counting the five spots on each mirror (10 pass for a total path of 55 cm). Focusing and beam spot size was qualitatively checked by this method. The 1.87-μm DFB laser had properties similar to those of the 1.37-μm laser and somewhat lower output power and was used in conjunction with an extended AlGaAs detector.

The mechanical fit was checked by mounting the whole spectrometer inside an aluminum tube section that was identical in I.D. and O.D. to the Pascal flight probe section. The aluminum cylindrical section of the probe was 3.25 in. long and weighed 0.60 lb (272.4 g). Subtracting this weight from the weight of the complete final assembly produced an instrument weight (all components including bracketry and mounting bolts) of 0.50 lb (227 g). Of this, the

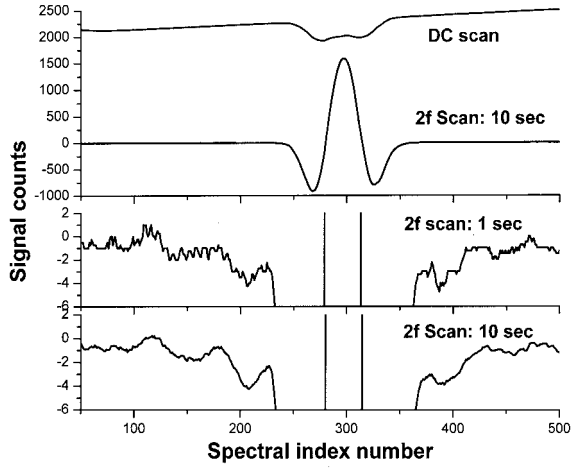

Fig. 6. Sensitivity study results for the 1.37-μm water line.

stuffed electronics board with no cabling weighs ~44 g.

While it was operating completely in the measurement cycle and scanning through the water line, the instrument was placed in a pressure vessel and the atmosphere about it was reduced to a pressure that simulated that of Mars, namely, ~7 mbars. The pressure-broadened linewidth was reduced significantly to expected values, and the instrument continued to perform excellently under these low-pressure conditions.

Although the Pascal laser hygrometer was designed for use only with a 5-V dc power supply, we also had to use a 12-V supply for a small logic component. During power-up the 5-V supply drew 982 mA of current. After less than 1 min the system was running continuously, drawing only 570 mA. The 5-V dc main supply therefore drew 5 W of power at start-up and 2.85 W running continuously. The 12-V supply drew only 2.5 mA and therefore consumed only 30 mW of power. Start-up power draw could be reduced at the expense of extending the warm-up time.

Figure 6 shows data from the 1.37-μm water line. The result of averaging four scans shows that white noise is a significant component of the 1-s data. The 38-scan average, representing 10 s of data, is clearly limited only by fringes. With a full 2*f* line of ~2400 counts, we identify two regions, namely, a cleaner region from 50–100 index counts where the peak-to-peak noise is 0.48 count and a region dominated by larger fringes near 100–200 index counts where the peak-to-peak noise is 1.5 counts. Therefore the minimum-detectable absorption level ranges from 3×10^{-5} to 8×10^{-5}. Transferring this measured sensitivity of $\sim 5 \times 10^{-5}$ to the 5327-cm^{-1} line near 1.8772 μm corresponds to an expected minimum-detectable mixing ratio for water vapor at 7 mbars and 170 K of ~1 ppmv (see Table 3).

At 1.87 μm the predicted absorption depth of the water line at 5327 cm^{-1} is 4×10^{-5} for 1-ppmv water in 7-mbar CO_2 at 170 K in the 55-cm path, according to the HITRAN spectral parameters. Repeating the laboratory measurements of sensitivities given above for this 5327-cm^{-1} line produced better results. A minimum-detectable absorption level of 2×10^{-5} was achieved in a single scan of 0.26 s, with a level of $\sim 5 \times 10^{-6}$ for a 10-s average. These results are better than those at 1.37 μm for two principal reasons: improved optical alignment to reduce fringes and a more-powerful laser source. The minimum-detectable absorption measured at 1.87 μm therefore corresponds to minimum-detectable mixing ratios for water vapor at 7 mbars of ~0.5 ppmv in a single scan of 0.26 s and of 0.1 ppmv in a 10-s measurement time (Table 3). This is equivalent to only $0.2–1.0 \times 10^{11}$ molecules/cm^{-3} of water, i.e., corresponds to a surface water frost-point temperature of approximately 160–165 K at a nominal surface pressure near 7 mbars.

Table 3. Instrument Sensitivity Results

Wavelength Region (μm)	Minimum-Detectable Volume Mixing Ratio Achieved (ppmv)	
	0.26-s Single Scan	10-s Average (38 scans)
1.37	1.6	1
1.87	0.5	0.1

E. Measurement Limitations

Like that of all tunable laser spectrometers, the sensitivity of this instrument is limited by optical interference fringes generated by weak reflections between optical elements. The worst fringe periods are those close to the linewidths or half-widths because they are the most difficult to remove through filtering or by postflight data fitting.[25] For the H_2O and CO_2 lines here [Fig. 2(b)], these are fringes with periods of approximately 0.01–0.02 cm^{-1}, which are associated with corresponding air path lengths of 20–60 cm (ZnSe path lengths of ~40% of these values are unlikely the cause). With good optical design (antireflection coatings, wedge windows, etc.) and careful alignment, fringes may appear only at absorption levels below $\sim 1 \times 10^{-5}$ for short integration times (seconds), and, as in our case described above, be reduced to 5×10^{-6} for a 10-s average. But the ability to reduce optical fringing (and therefore to increase sensitivity) by increasing integration time is limited, and it depends on environmental conditions. In the changing temperatures of our laboratory, residual fringes were clearly moving in absolute wave number and averaging out with time, as we saw with our improvement in going from a 1- to a 10-s average, but this may not be true in a stable Martian environment. However, with large diurnal changes in Martian temperature, and with changing instrument on–off sequencing activities, we expect to see fringe averaging to some extent.

Concerning absolute accuracies for the measurement of water vapor mixing ratios, experience with

preflight calibration of Earth instruments by use of frost-point hygrometers suggests that ~5% is a reasonable estimate of absolute error. However, if the Mars ambient pressure were separately measured to 1%–2% uncertainty, and the temperature to 2 K, then we could derive the CO_2 number density and use the CO_2 line adjacent to that of H_2O (Fig. 2) to improve the absolute accuracy for the H_2O measurement, possibly to 97%–98%.

Making precise and accurate measurements of water on Mars will need particular attention to sampling issues that plague all *in situ* measurements on Earth to various degrees, especially at low mixing ratios. Whereas the spectroscopic technique of the MLH is highly species specific, it is not impervious to contamination from other water sources or by errors that result from wall surface artifacts such as outgassing and surface adsorption. Diurnal patterns in Martian water vapor driven by solar heating must not be confused with outgassing of water vapor that has adhered to instrument surfaces at night. For a Mars lander, rover, or surface station, although the complete payload will have outgassed water on its long journey to Mars, all surfaces (e.g., insulation) could breathe water in synchronization with the diurnal atmospheric cycle. It is critical to eliminate these memory effects if accurate high response time flux measurements are to be made, and special provisions for eliminating these effects must be made. Materials used for exposed surfaces should first be carefully selected (although heavier stainless steel or nickel are better choices than aluminum or titanium, both of which form relatively sticky oxide layers) and then treated if necessary. Before measurement it may be necessary to heat the instrument well above ambient temperature to remove adhered water and then to let the instrument settle long enough at ambient temperature to allow the walls to take up water as equilibrium is achieved. A measurement cycle strategy will need to be developed that includes engineering data to help identify contamination.

Finally, the extent to which Martian dust can degrade measurement ability or accuracy is estimated. A strength of TDL absorption measurement is that it be self-calibrating in the sense that through Beer's law water abundances can be calculated despite diminishing of laser power through misalignment or optical losses. In fact, the 1.87-μm TDL used has enough power (several milliwatts) to permit significant loss of power (~1 order of magnitude) before accuracy and precision are seriously compromised. However, when laser power diminishes to the point that the measurement is no longer fringe limited, precision will be reduced proportionally to laser power loss. Some of this precision can be recovered with increased integration time if the measurement strategy or the science requirements allow. Martian dust falling onto the mirror surfaces will reduce the optical throughput quickly, because in the multipass arrangement the throughput drops as the effective reflectivity (R_{eff}) to the power of the number of passes. For $R_{\text{eff}} = 0.95$, a 10-pass cell will allow ~60% of the light to reach the detector, but with Martian dust reducing R_{eff} to 0.5, the light on the reflector will be reduced to only ~0.1% of the incident light. Because laser beam diameters on the mirror are much larger than dust particle size, this reduction will occur when a fine single layer of dust is formed that is equivalent to approximately half of the area of the mirror. As in all *in situ* optical measurement techniques for Mars, strategies for minimizing dust contamination must be employed. This could include a dust–air fine filter across the open cradle of the cell.

In summary, a prototype laser hygrometer has been fabricated, integrated, and tested for fit-check, laser-detector operation, optical alignment, Mars pressure operation, and spectral sensitivity. It has achieved a sensitivity (precision) of measuring water vapor down of one tenth of one part in 10^6 by volume (0.1 ppmv) in a 10-s measurement time at a nominal surface pressure near 7 mbars, which would be equivalent to 2×10^{10} molecules cm^{-3}, i.e. a surface water frost-point temperature of ~160 K. The complete instrument weights only 230 g and consumes <3 W of power when it is running. Further development of flight qualification of lasers at 1.87 μm, identifying a radiation-hardened version of the HC12 microcontroller, and extended g-force testing are needed before deployment of the hygrometer on Mars.

This research was performed at the Jet Propulsion Laboratory, California Institute of Technology, under a contract with the National Aeronautics and Space Administration. The following people contributed to the instrument development and laboratory prototyping: Chris Webster, instrument concept, overall design, spectroscopy, testing, sensitivity analysis, and reporting; Gregory J. Flesch, data processing, instrument control software, and electronics troubleshooting; Linley Kroll, detailed mechanical design; Ron Howe, machining of parts; Steve Woodward, electronics design; Jim Swanson, electronic board layout and assembly; and Bob Bamford, high-g design analysis.

References and Notes

1. G. J. Taylor, A. Morrison, and D. Beaty, "Mars Exploration Program Analysis Group (MEPAG) report: scientific goals, objectives, investigations, and priorities: 2003," http://mepag.jpl.nasa.gov/reports.
2. R. M. Haberle, "The science return of a global surface network on Mars: the Pascal Mars Scout concept," presented at the Aerospace Conference, IEEE Meeting, Big Sky, Montana, 8–15 March, 2003), bhaberle@mail.arc.nasa.gov.
3. R. W. Zurek, J. R. Barnes, R. M. Haberle, J. B. Pollack, J. E. Tillman, and C. B. Leovy, "Dynamics of the atmosphere of Mars," in *Mars*, H. H. Kieffer, B. M. Jakosky, C. W. Snyder, and M. S. Matthews, eds. (U. Arizona Press, Tucson, Ariz., 1992), Chap. 26.
4. R. A. Kahn, T. Z. Martin, R. W. Zurek, and S. W. Lee, "The Martian dust cycle," in *Mars*, H. H. Kieffer, B. M. Jakosky, C. W. Snyder, and M. S. Matthews, eds. (U. Arizona Press, Tucson, Ariz., 1992), Chap. 29.
5. T. Owen, "The composition and early history of the atmosphere of Mars," in *Mars*, H. H. Kieffer, B. M. Jakosky, C. W. Snyder,

and M. S. Matthews, eds. (U. Arizona Press, Tucson, Ariz., 1992), Chap. 25.
6. L. K. Tamppari, A. S. Hale, D. S. Bass, and M. D. Smith, "Using MGS data to understand water cycling in Mars' north polar region," Lunar Planet. Sci. **34,** 1650–1651 (2003).
7. I. G. Mitrovanov, M. T. Zuber, M. L. Litvak, W. V. Boynton, D. E. Smith, D. Drake, D. Hamara, A. S. Kozyrev, A. B. Sanin, C. Shinohara, R. S. Saunders, and V. Tretyakov, "CO_2 snow depth and subsurface water-ice abundance in the northern hemisphere of Mars," Science **300,** 2081–2084 (2003).
8. C. B. Farmer, D. W. Davies, and D. D. LaPorte, "Mars: northern summer ice cap-water vapor observations from Viking 2," Science **194,** 1339–1341 (1976).
9. M. C. Malin and K. S. Edgett, "Evidence for recent groundwater seepage and surface runoff on Mars," Science **288,** 2330–2335 (2000).
10. R. M. Haberle, C. P. McKay, J. Schaeffer, N. A. Cabrol, E. A. Grin, A. P. Zent, and R. Quinn, "On the possibility of liquid water on present-day Mars," J. Geophys. Res. **106,** 23,317–23,326 (2001).
11. S. Byrne and A. P. Ingersoll, "A sublimation model for Martian south polar ice features," Science **299,** 1051–1053 (2003).
12. World Meteorological Organization, "Stratospheric processes and their role in climate (SPARC) assessment of UT/LS water vapour," Rep. WCRP-113 (World Meteorological Organization, Geneva, 2000).
13. See the JPL website, http://laserweb.jpl.nasa.gov.
14. R. D. May, S. F. Forouhar, D. Crisp, W. S. Woodward, D. A. Paige, A. Pathare, and W. V. Boynton, "The MVACS tunable diode laser spectrometers," J. Geophys. Res. **106,** 17,673–17,682 (2001).
15. J. Faist, F. Cappasso, D. L. Sivco, C. Sirtori, A. L. Hutchinson, and A. Y. Cho, "Quantum cascade laser," Science **264,** 553–556 (1994).
16. C. Gmachl, A. Straub, R. Colombelli, F. Capasso, D. L. Sivco, A. M. Sergent, and A. Y. Cho, "Single mode, tunable distributed-feedback and multiple wavelength quantum cascade lasers," IEEE J. Quantum Electron. **38,** 569–581 (2002).
17. C. R. Webster, G. J. Flesch, D. C. Scott, J. Swanson, R. D. May, W. S. Woodward, C. Gmachl, F. Capasso, D. L. Sivco, J. N. Baillargeon, A. L. Hutchinson, and A. Y. Cho, "Quantum cascade laser measurements of stratospheric methane and nitrous oxide," Appl. Opt. **40,** 321–326 (2001).
18. M. Beck, D. Hofstetter, T. Aellen, J. Faist, U. Oesterle, M. Ilegems, E. Gini, and H. Melchior, "Continuous wave operation of a mid-infrared semiconductor laser at room temperature," Science **295,** 301–305 (2002).
19. C. R. Webster, R. T. Menzies, and E. D. Hinkley, "Infrared laser absorption: theory and applications," in *Laser Remote Chemical Analysis*, R. M. Measures, ed. (Wiley, New York, 1988), Chap. 3.
20. L. S. Rothman, A. Barbe, D. C. Benner, L. R. Brown, C. Camy-Peyret, M. R. Carleer, K. Chance, C. Clerbaux, V. Dana, V. M. Devi, A. Fayt, J.-M. Flaud, R. R. Gamache, A. Goldman, D. Jacquemart, K. W. Jucks, W. J. Lafferty, J.-Y. Mandin, S. T. Massie, V. Nemtchinov, D. A. Newnham, A. Perrin, C. P. Rinsland, J. Schroeder, K. M. Smith, M. A. H. Smith, K. Tang, R. A. Toth, J. Vander Auwera, P. Varanasi, and K. Yoshino, "The HITRAN molecular spectroscopic database: edition of 2000 including updates through 2001," J. Quant. Spectrosc. Radiat. Transfer **82,** 5–44 (2003).
21. MayComm Instruments, llc; see http://www.MayComm.com.
22. D. R. Herriott, H. Kogelnik, and R. Kompsner, "A scanning spherical mirror interferometer for spectral analysis of laser radiation," Appl. Opt. **3,** 1471–1484 (1964).
23. NASA parts selection list; see http://nepp.nasa.gov.
24. S. W. Woodward and R. D. May, "Flash-ROM-based multichannel arbitrary-waveform generator," Electron. Design 19 April, 86–88 (1999), http://www.elecdesign.com/Articles/ArticleID/6220/6220.html.
25. C. R. Webster, "Brewster-plate spoiler: a novel method for reducing the amplitude of interference fringes that limit tunable laser absorption sensitivities," Appl. Opt. **2,** 1464–1470 (1985).